BUCK AND BOOST CONVERTER BASED 2-PV IN MISMATCHED CONDITIONS FOR SPGCT INVERTER

Dr. Sankar Babu Potluri, Professor and HoD, EEE Department, SVR Engineering College, Nandyal
Gaja Chandra Sekhar, Asst. Professor, EEE Department, SVR Engineering College, Nandyal

Abstract—1-ϴ grid connected transformer that can work in either a buck or boost mode with a less photo voltaic (PV) inverter, and that can simultaneously derive full power from two serially connected subarrays when each subarray faces different environment conditions, is introduced in this paper. Since the inverter can act both in buck and boost mode based on specifications, it significantly reduces the restriction on the minimum number of serial attached solar pv modules required for forming a subset. As a consequence, the power output of each subfield increases when subjected to varying environmental conditions. The topological structure and the control strategy of the inverter are designed to avoid high frequency components being present in the typical mode voltage, thereby limiting the degree of the PV arrays' leakage current within the stated limit. In comparison, high operational performance is obtained across its spectrum. The mechanism leading to the development of its mathematical model is studied in depth. Detailed modelling experiments confirm the feasibility of the scheme.

Index Terms—Grid connection, 1-phase, Transformer less, Buck and Boost, MPPT.

I. INTRODUCTION

A Photo Voltaic (PV) system is mainly concerned with ensuring optimal efficiency for and PV modules in a PV series, since the modules are prone to differing external factors due to differences in insolation levels and/or variations in operating temperature. The existence of malfunctions in the working state of modules decreases the PV performance substantiallyThe Mismatched Environmental Conditions (MEC) issue is significant since there are a large number of sequentially related modules in the PV series. To obtain the desired magnitude for the input DC connecting voltage of the inverter of a grid connected transformer less PV system, the requirement for series-connected modules is strong. Inverter-based H-bridge and Neutral Point Clamp (NPC) inverter devices, such as the Single Phases GCT (SPGCT) performance, are also dramatically affected by MEC. Various solutions in the literature are documented to resolve the problem emerging from MEC in a PV environment. Elective connectivity between PV modules or global tracking of the Maximum Power point (MPP) of the PV array can be improved during MEC using a complex MPP Tracking (MPPT) algorithm. However these methods do not work for the low-power SPGCT PV system. Similarly, it is not productive to reconfigure PV modules in a PV array by modifying the electrical relation of PV modules for the SPGCT PV system as components are substantially increased and organisational complications increase.

During MEC per PV module of a PV series was operated using a power equaliser or a DC to DC converter for optimum performance from each PV module. Schemes using electronic equalizers require vast quantities of components to increase the device expense and operating complexity. The scheme implemented in the Control Circuit Generation (GCC) uses each PV module for their respective MPP, whereby the power differential between each module is only processed via the GCC.

This scheme uses shunt current compensation for each module and series-voltage compensation for each PV string inside a PV array to increase the energy performance of MEC. Dc to dc integrated with and PV module was added to the integrated module converter-based systems. However, owing to the participation of a large number of converter steps, the performance of the above schemes is poor and furthermore the device count is strong and hence they experience similar drawbacks to the power electronic equaliser system. Instead of ensuring MPP function of each node, a number of modules are attached to a string in sequence, and then shaped strings are used under MPP. Even though, total part count and control sophistication are not substantially reduced.

In order to simplify the control setup and reduce the number of components, the schemes mentioned integrate all PV modules in two subfunctions, and then each of the subfunctions is run on its own MPP. The overall performance of both schemes recorded however is low. The buck and boost stage of the

SPGCT PV inverter improves power extraction during MEC. Furthermore, the need for series attached PV modules in the PV array has decreased due to the inclusion of the intermediate boost stage.

The schemes provided work at high frequencies with either the dc to dc conversion stage or the inverter stage; as a consequence, the size of the passive part count has decreased considerably and the operation performance of these schemes has been improved. In addition, the stated efficiency is 1-2% higher than that of. This article aims to divide the PV- modules into two serially-connected subfields and to monitor each subfield using a buck- and boost-based inverter to verify an efficient power evacuation from the subfields during MEC.

The proposed inverter's topological structure and management method Ensure that the PV array leakage current stays under the allowed cap. The voltage voltage of the operating instruments is reduced by around half compared to the presented schemes, thereby ensuring very high frequency activity without growing switching failures. High frequency processing also decreases the size of passive components. The operational performance of the suggested scheme is also strong.

The measured peak performance and European efficiency (αeuro) of the planned scheme are 97.65% and 97.02% respectively.

The productivity of the proposal presented is strong. The intentional efficacy pinnacle and European efficiency (αeuro) of the planned system is 97.65% and 97.02%.

II.   PHOTOVOLTAIC CELL

A PV cell is a simple p-n intersection diode which transforms into power over light. Fig.1 outlines a direct analogous PV cell circuit diagram. The current source speaks of the PV cell produced current, a diode in parallel with the current source, a shunt obstacle, and series resistance.
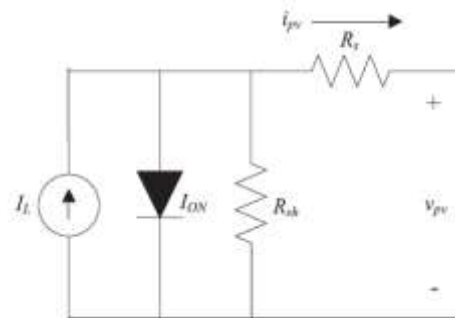
Fig.1 Equivalent circuit diagram of the PV cell

III.   DC-DC CONVERTERS

A high-voltage DC-DC converter that can be used in numerous applications such as vehicle headlights, power module vitality transition mechanisms, cell sun-based cell life transformation framework systems, and battery strengthening frames for continuous power supplies. A dc-dc Converter can potentially reach a high advanced voltage with a high effective obligation ratio. However the advance voltage gain is limited to the influence of strength switches and the relative resistance (ESR) of inductors and condensers.

BUCK-BOOST CONVERTERS:

An essential buck-support converter is appeared in Fig 2. This converter's latest knowledge current can be contained in its current data waveform.

The equation indicates the average time period present (t) $I_{1, avg}(t) = D^3 T_s / 3L \, V_1(t)$
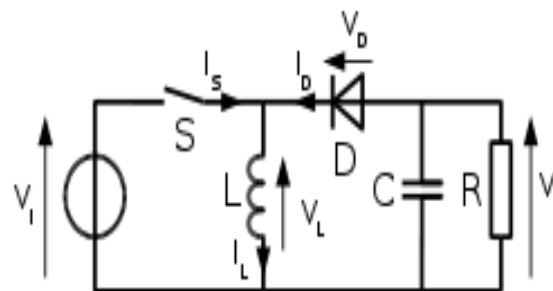
Fig: 2. Buck –Booster Converter

IV. INVERTER AND ITS OPERATION

The scheme shown in Fig.3 of the proposed Dual Buck & Boost Inverter (DBBI) consists of a dc to dc conversion step and then a reversing stage. The stage dc to dc converter has two segments of DC to DC converters CONV1 and CONV2 to support the solar pv array's two subsets PV1 and PV2. The CONV1 segment consists of S1 self-switched switches along with its D1, S3 anti-parallel body diode and an anti-parallel body diode D3, Df1, Df3 and L1 philtre inducers and condensers. Similarly, the CONV2 section is made up of autocommuting switches, S2 with an anti-parallel body diode, D2, S4 with an anti-parallel body diode, D4 with freewheelers, Df2, Df4 and philtre inducers and condensers, D2, Cf2 and Co2. The invert step consists of S5, S6, S7, S8 and the associated body diodes, D5, D6, D7 and D8 self-commuted switches. The philter inductor, Lg, binds the inverter stage to the grid. The PV panel for ground parasite capacitance is modelled on condensers Cpv1 and Cpv2.
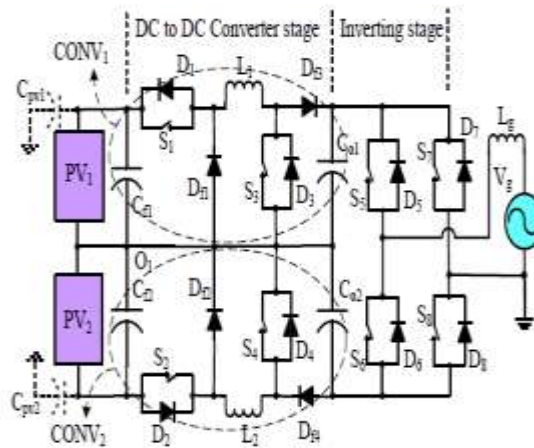
Fig.3. Dual Buck and Boost based Inverter (DBBI)
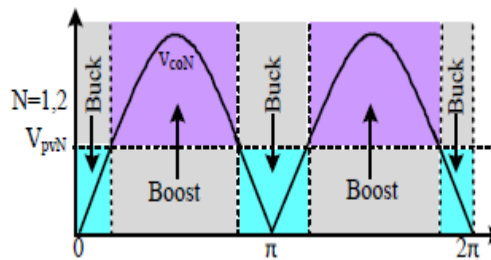
Fig.4. Buck-Boost Stage of the inverter

Taking into consideration Fig. Vpv1, Vpv2 are PV1 and PV2 MPP, and vco1, vco2 are all CONV1 and CONV2 performance voltages. The S1 and S2 are separate sinusoidally during the service ratios of the buck mode transitions, maintaining sinusoidal grid current (ig) when S3 and S4 are held off. If Vpv1 < vco1, CONV1 works in boost mode when CONV2 works in booster mode when Vpv2 < vco2. S3 and S4 are variatedsinusoidally during the boost mode of the switches to ensure sinusoidal ig whereas S1 and S2 are held in the whole mode. The sinusoidal pulses of the CONV1 and CONV2 switches are synchronised with the grid voltage, vg for the application of the device power factor. Switching, S5 and S8 are retained and S6 and S7 switches are held out for the whole positive half cycle, while switches S6 and S7 are kept on and off, while S5 and S8 are permanently left off over the entire pessimistic half cycle (NHC). Fig.4. Where the insolation levels and atmospheric temperature of the sub array PV1 vary from those of PV2, the MPP parameters are reflected in all the operating conditions of the proposed inverter.
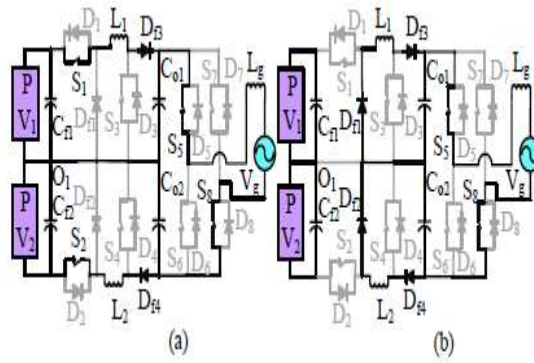
(a) Active & (b) Freewheeling states in of PHCbuck mode
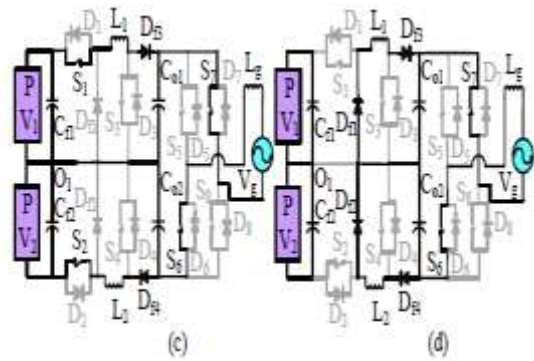
(c) Active & (d) Freewheeling states in NHC buck mode
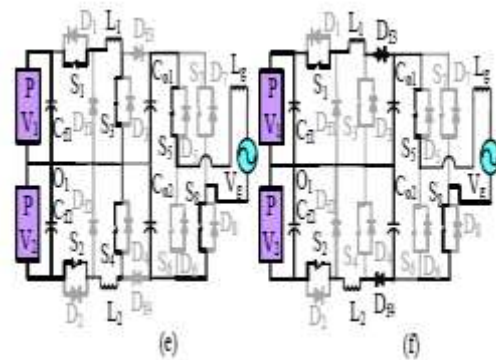
(e) Active & (f) Freewheeling states in PHC boost mode
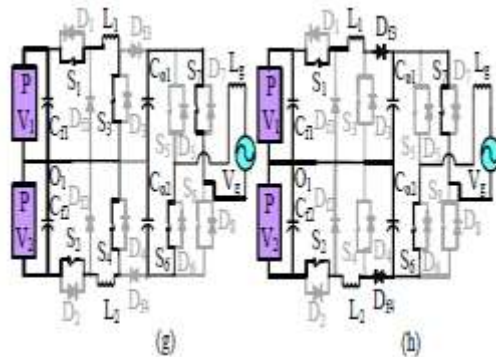
(g) Active & (h) Freewheeling states in NHC boost mode

Fig.5. Operating states of DBBI

Of the two separate subarrays, Vpv1 and Vpv2, the present MPP, Ipv1 and Ipv2 are respectively PV1 and PV2, and the strength of MPP, Ppv1 and Ppv2 is PV1 and PV2 respectively. Provided that all sub-arrays run on the respective MPS, and that power processing losses are ignored, the average power of Co1 and Co2, Pco1 and Pco2, over a half-cycle, is equivalent to the power of PV1 and PV2, respectively.

$$Pco1 = Ppv1 \ \& \ Pco2 = Ppv2 \qquad \text{.... (1)}$$

The power that is pumped into the grid over a half period is Pg

$$Pg = Ppv1 + Ppv2 \qquad \text{.... (2)}$$

Further, at any half cycle

vg= vco1 + vco2   .... (3)

Therefore, the instant inject power into the gridpg can be written as

pg= vgig= (vco1 + vco2)ig   ....(4)

Where the instantaneous amounts of Vco1 and Vco2 are indicated in vco1 and vco2 respectively. As ig is in the vg process,

$$I_g = \frac{P_g}{V_g} \qquad \text{.... (5)}$$

Where in Vg and Igrms represent vg and ig values respectively.

The power can be represented when pumped into the grid

$$
\begin{aligned}
P_g &= \frac{1}{\pi}\int_0^\pi p_g\, d(\omega t) \\
&= \frac{1}{\pi}\int_0^\pi v_{co1} i_g\, d(\omega t) + \frac{1}{\pi}\int_0^\pi v_{co2} i_g\, d(\omega t) \qquad \text{.... (6)}
\end{aligned}
$$

= Pco1 + Pco2   .... (7)

$$
\begin{aligned}
P_{co1} &= \frac{1}{\pi}\int_0^\pi V_{co1m}\sin(\omega t)\, I_{gm}\sin(\omega t)\, d(\omega t) \\
&= \frac{V_{co1m} I_{gm}}{2} \qquad \text{.... (8)}
\end{aligned}
$$

Similarly,

$$P_{co2} = \frac{V_{co2m} I_{gm}}{2} \qquad \text{.... (9)}$$

$$V_{co1m} = \frac{2P_{pv1}}{I_{gm}} = \frac{\sqrt{2}P_{pv1}}{I_g} = \frac{\sqrt{2}P_{pv1}}{P_g/V_g} \qquad \text{....(10)}$$

$$V_{co2m} = \frac{2P_{pv2}}{I_{gm}} = \frac{\sqrt{2}P_{pv2}}{I_g} = \frac{\sqrt{2}P_{pv2}}{P_g/V_g} \qquad \text{.... (11)}$$

Similarly by combining (2), (10) and (11),

$$V_{co1m} = \frac{V_m P_{pv1}}{P_{pv1}+P_{pv2}} \quad \& \quad V_{co2m} = \frac{V_m P_{pv2}}{P_{pv1}+P_{pv2}} \qquad \text{.... (12)}$$

The vco1 and vco2 voltage models behave as full-wave sinusoidal, Vco1m and Vco2m amplitudes. Vm is the vg amplitude. The magnitudes of Vco1m and Vco2m can be deduced from (12) by the strength derived from each sub series. If the PV1 power is less than PV2, the Vco1m is less than Vco2m, whereas the

$$d_{1m} = \frac{V_{co1m}}{V_{pv1}} \quad \& \quad d_{2m} = \frac{V_{co2m}}{V_{pv2}}$$

Vco2m is less than PV1 with PV2.   .... (13)

In boost mode, the job ratios of d3 of S3 and d4 of S4 differ with amplitude d3m and d4m and with

$$d_{3m} = 1 - \frac{V_{pv1}}{V_{co1m}} \quad \& \quad d_{4m} = 1 - \frac{V_{pv2}}{V_{co2m}}$$

amplitude d4m. .... (14)

The CONV1 and CONV2 are equally efficient. Thus before input filtering by CONV1, isw1 and CONV2 input philtre condenser, isw2 can be correlated with ig in the buck mode by considering the average swapping time of the respective amounts as follows.

$$\langle i_{sw1} \rangle_{T_s} = \langle d_1 \rangle_{T_s} \langle i_g \rangle_{T_s}$$ .... (15)

$$\langle i_{sw2} \rangle_{T_s} = \langle d_2 \rangle_{T_s} \langle i_g \rangle_{T_s}$$ .... (16)

Similarly, the relation between isw2, isw1 &ig can be extracted during boost mode by considering the

$$\langle i_{sw1} \rangle_{T_s} = \langle \frac{1}{1 - d_3} \rangle_{T_s} \langle i_g \rangle_{T_s}$$

switching period average of the respective quantities .... (17)

$$\langle i_{sw2} \rangle_{T_s} = \langle \frac{1}{1 - d_4} \rangle_{T_s} \langle i_g \rangle_{T_s}$$ .... (18)

Taking into consideration Fig. It should be remembered that vcpv1 = vco2 + Vpv1, vcpv2 = vco2 - Vpv2, during the PHC activities, whereas NHC vcpsv1 = vco1 + Vpv1, vcpv1 = -vco1 - Vpv2, with voltages impressed by Cpv1 and Cpv2, respectively, in vcpv1 and vcpv2. The voltages of Cpv1 and Cpv2 also include substantial amounts of dc and low frequency components that often ensure that the leakage current magnitude is kept within the limits of the norm.

V. SIMULATION STUDIES

A PV array consisting of two PV subarrays is considered to show the efficiency of the proposed inverter when each of these subarrays comprises four series of linked Canadian solar polycrystalline modules. The normal test state in the MPP of each sub-array (STC) is Vpv1 = 116 V. Table1 the Matlab-simulink platform uses the parameters that simulate the proposed inverter to simulate the inverter performance. The insolation and temperature variations known for the performance of the proposed inverter in both sub-ranges.

The Ppv1, Ppv2, Vpv1, Vpv2 variations in both subarrays and the ability to concurrently operate both subarrays with their respective MPP Fig.5.1a & 5.1b of the proposed inverter. Figures 4-6 indicate variations in ig, iL1, iL2, vco1 and vco2 and extended variants for two different sunscreens.
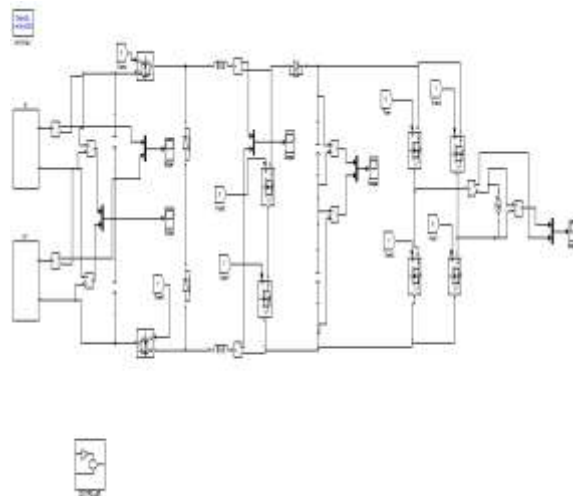
Fig..6. Simulation Diagram for Dual Buck and Boost based Inverter
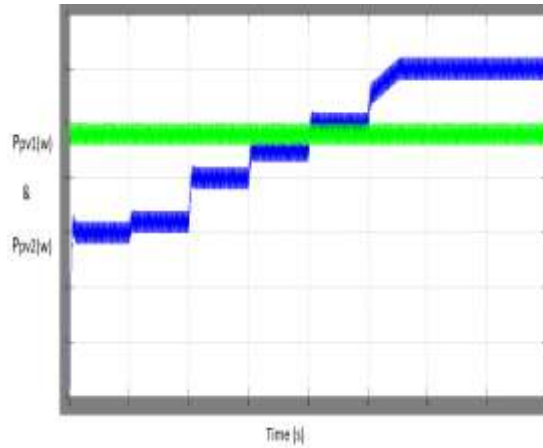
Fig.7. Simulated Waveform: Variation in Ppv1 and Ppv2
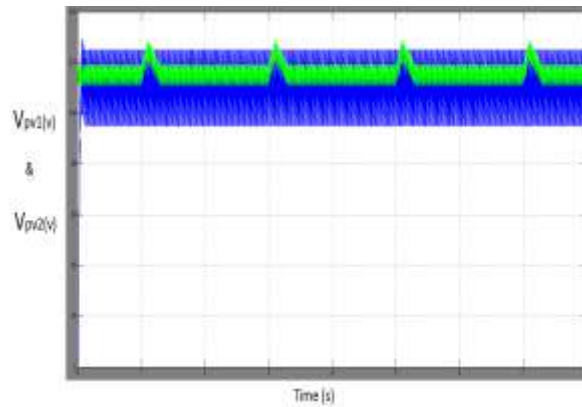
Fig.8. Simulated Waveform: Variation in Vpv1 and Vpv2 during entire range of operation
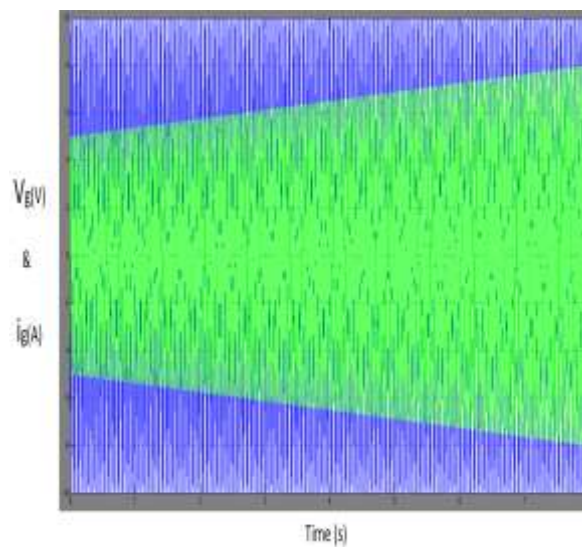
Fig.9. Simulated Waveform: Vg and ig
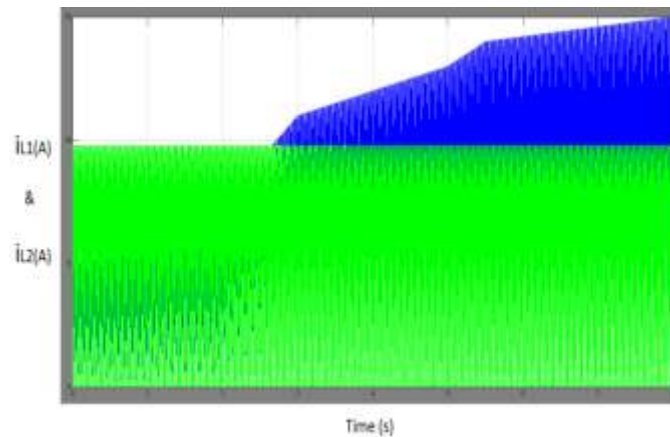
Fig.10. Simulated Waveform: iL1 and iL2
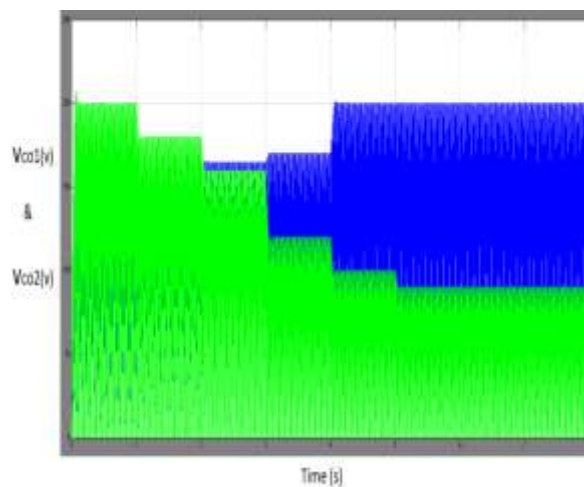
Fig.11. Simulated Waveform: Vco1 and Vco2

VI. CONCLUSION

This paper suggests a single stage matrix of the transformer with fewer buck and a lift-based PV inverter that can operate on two substrates with its different MPP. I) the influence of fudged natural conditions on the PV cluster could be controlled in an insistent manner, ii) job capability was achieved, β = 97.02 per cent was strong, iii) the decoupled component regulation was conceivable, iv) clear MPPT measurement was used to ensure MPP operation for segment converters, v) spillage currencies. The highlight of this inverter was: The scientific analysis of the proposed inverter was performed to develop its small sign model. The rule for selecting the estimates of the yield channel segments was seen. The proposal was accepted with the use of specific recreation experts and the reasonableness of the plan was thus defined through extensive exploratory testing on a 1.5 kW inverter configuration.

REFERENCES

[1]T. Shimizu, O. Hashimoto, and G. Kimura, "A novel high-performance utility-interactive photovoltaic inverter system," IEEE Trans. Power Electron., vol. 18, no. 2, pp. 704-711, Mar. 2003.

[2] S. V. Araujo, P. Zacharias, and R. Mallwitz, "Highly efficient single phase transformer less inverters for grid-connected photovoltaic systems," IEEE Trans. Ind. Electron., vol. 57, no. 9, pp. 3118-3128, Sep. 2010.

[3] B. Ji, J. Wang, and J. Zhao, "High-efficiency single-phase transformer less PV H6 inverter with hybrid modulation method," IEEE Trans. Ind. Electron., vol. 60, no. 5, pp. 2104-2115, May 2013.

[4] R. Gonzalez, E. Gubia, J. Lopez, and L. Marroyo, "Transformer less single phase multilevel-based photovoltaic inverter," IEEE Trans. Ind. Electron., vol. 55, no. 7, pp. 2694-2702, Jul. 2008.

[5] H. Xiao and S. Xie, "Transformer less split-inductor neutral point clamped three-level PV grid-connected inverter," IEEE Trans. Power Electron., vol. 27, no. 4, pp. 1799-1808, Apr. 2012.

[6] A. Bidram, A. Davoudi, and R. S. Balog, "Control and circuit techniques to mitigate partial shading effects in photo voltaic arrays," IEEE J. Photovolt., vol. 2, no. 4, pp. 532-546, Oct. 2012.

[7] N. D. Kaushika, and N. K. Gautam, "Energy yield simulations of interconnected solar PV arrays," IEEE Trans. Energy Convers., vol. 18, no. 1, pp. 127-134, Mar. 2003.

[8] H. Patel, and V. Agarwal, "Maximum power point tracking scheme for PV systems operating under partially shaded conditions," IEEE Trans. Ind. Electron., vol. 55, no. 4, pp. 1689-1698, Apr. 2008.

[9] D. Nguyen, and B. Lehman, "An adaptive solar photovoltaic array using model-based reconfiguration algorithm," IEEE Trans. Ind. Electron., vol. 55, no. 7, pp. 2644-2654, Jul. 2008.

[10] G. V.-Quesada, F. G.-Gispert, R. P.-Lopez, M. R.-Lumbreras, and A. C.- Roca, "Electrical PV array reconfiguration strategy for energy extraction improvement in grid-connected PV systems," IEEE Trans. Ind. Electron., vol. 56, no. 11, pp. 4319-4331, Nov. 2009.